Grain growth in systems with anisotropic boundary mobility: Analytical model and computer simulation

A. Kazaryan
Department of Physics, The Ohio State University, Columbus, Ohio 43210

Y. Wang and S. A. Dregia
Department of Materials Science and Engineering, The Ohio State University, Columbus, Ohio 43210

Bruce R. Patton
Department of Physics, The Ohio State University, Columbus, Ohio 43210

(Received 18 August 2000; revised manuscript received 19 December 2000; published 17 April 2001)

We investigate the effect of anisotropy in grain boundary mobility on the dynamics, morphology, and topology of grain growth, using both analytical and numerical calculations on a generalized anisotropic phase field model. The dependence of the grain boundary mobility on both inclination and misorientation is included. In contrast to the isotropic case, where a single grain in a polycrystalline system grows linearly with time, it is found that the growth rate of a single *n*-sided grain in the anisotropic case is time dependent. The growth rate of the average area is also time dependent, except for the two limiting cases of textured and randomly oriented grain structures. However, strong grain shape anisotropy develops in the textured case, indicating that the grains grow in a non-self-similar manner. In the intermediate case, the deviation from a growth exponent of unity is of order 10%, while the size and edge distributions are similar to those of the isotropic system. Our results indicate that statistical self-similarity may not be required for linear growth kinetics and time-invariant size and edge distributions.

DOI: 10.1103/PhysRevB.63.184102 PACS number(s): 81.15.Aa, 68.55.−a, 05.45.−a

I. INTRODUCTION

Grain growth is an interesting and important problem, which controls a number of physical and mechanical properties of polycrystalline materials. It has been extensively studied for decades using a variety of theoretical and experimental approaches (see Refs. 1–5 for recent reviews). However, most of the studies so far have been devoted to understanding grain growth behavior in the isotropic limit, i.e., when both energy and mobility of the grain boundaries are isotropic. The reason behind it lies in the self-similarity approximation (all configuration have identical statistics when transformed to the same linear scale by uniform magnification) that brings significant simplifications into the analysis of the problem. However, both energy and mobility can be strongly anisotropic, e.g., their values depend on the misorientation between two neighboring crystals and the spatial orientation (inclination) of the boundaries.[6,7] In addition, phenomena such as segregation of impurities[5,8] or presence of liquid phase[9] at the grain boundaries may also result in strong anisotropy of both energy and mobility. However, the simplifying assumption self-similarity may not hold when boundary properties (energy and/or mobility) are anisotropic.[10]

Due to the complexity of the problem there is an increasing interest in using computer simulations to study grain growth in single and multiple phase materials. Although most computer simulations of grain growth have been performed for the isotropic case,[11–16] grain boundary anisotropy has been introduced in a number of simulations.[17–26] In the studies of texture development and texture controlled grain growth,[17–21] grains are divided into two types (A and B) which form three types of grain boundaries, corresponding to either small or large misorientations. For example, boundaries between grains of type A ($A-A$ boundaries) and type B ($B-B$ boundaries) are small angle boundaries and are assumed to have much lower energy and mobility than the high angle $A-B$ boundaries. To take into account the full range of misorientations, more general models have been proposed.[22–26] However, all these models consider only misorientation or inclination dependence of grain boundary properties. In general, energy and mobility of grain boundaries should depend on both misorientation and inclination.[27] Furthermore, in the models that deal with inclination dependence[24,25] only a few inclinations are considered and the use of only first neighbors for the calculation of boundary inclination results in an intrinsic energy and mobility anisotropy associated with the discrete lattice used in the simulations.[28]

In this paper we present both analytical and numerical investigations of grain growth in systems with anisotropic boundary mobility. We relate our analytical results to the treatment of Mullins in the isotropic limit.[10,29–31] Computer simulations are based on a generalized anisotropic phase field model that takes into account both misorientation and inclination dependence of the grain boundary energy and mobility. In the current paper we focus on the effect of grain boundary mobility anisotropy on the kinetics and morphology of grain growth. The effect of energy anisotropy as well as the interplay between the energy and mobility anisotropy will be discussed elsewhere.[32]

In the following section we present the generalized anisotropic phase field model. In Sec. III we discuss the effect of boundary mobility anisotropy on the shape and shrinkage kinetics of an island grain in an infinite matrix and show that

grain boundary mobility anisotropy can strongly influence the growth kinetics of a single grain in a polycrystalline aggregate. In Sec. IV we consider the kinetic, morphological and topological evolution of a polycrystalline microstructure. Major results are summarized in Sec. V.

II. GENERALIZED ANISOTROPIC PHASE FIELD MODEL

The phase field approach has been successfully used in computer simulations of dendrite formation during solidification,[33] multiphase and multidomain microstructural evolution during various solid state phase transformations,[34] and isotropic grain growth.[14,15] Here by ''isotropic'' we mean that both energy and mobility of grain boundaries in the system are constant. In the phase field model an arbitrary single phase polycrystalline microstructure is described by a set of nonconserved order parameter fields $(\eta_1, \eta_2, \ldots, \eta_p)$ representing grains with different crystallographic orientations. In contrast to the sharp interface approach where the variables describing the microstructure change instantaneously across the boundary, the field variables change continuously across the grain boundaries. Thus, the phase field model is often referred to as a diffuse-interface model. Microstructural evolution during grain growth is characterized by the spatio-temporal evolution of these order parameters via the Ginzburg-Landau type kinetic equations:

$$\frac{d\eta_i}{dt} = -L\frac{\delta F}{\delta \eta_i}, \tag{1}$$

where L is the kinetic coefficient that characterizes the grain boundary mobility and F is the free energy functional, which can be written in the following form:

$$F = F_0 + \int_V d^3r \left[f_0(\eta_1, \eta_2, \ldots, \eta_p) + \frac{k}{2}\sum_{i=1}^{p} \left|\nabla \eta_i\right|^2 \right], \tag{2}$$

where $f_0(\eta_i)$ is the free energy density and k is the gradient energy coefficient, which together determine the width and energy of the grain boundary regions.

A number of attempts have been made to introduce anisotropy of grain boundary properties into this formalism. For example, in the phase field models of antiphase domain motion and solidification, anisotropy has been introduced by using a set of order parameters based on the underlying crystal symmetries.[35,36] Since the structure of a grain boundary is much more complicated than that of a solid-liquid interface and its general description is still lacking, application of this approach to the description of grain growth remains a difficult challenge. Another way to introduce anisotropy into the phase field model has been recently proposed by Kobayashi *et al.*[37] and independently by Lusk,[38] where the microstructure is characterized by order parameters that describe the degree of crystallinity and crystalline orientation. In contrast to our model, where each orientation has its corresponding order parameter, this approach is computationally less intensive, but still does not include the inclination dependence of the grain boundary properties.

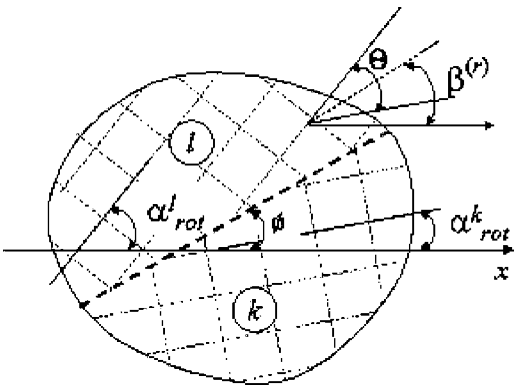

FIG. 1. Schematic drawing of a tilt grain boundary formed by two crystals l and k with misorientation θ and inclination ϕ, measured from the symmetric tilt boundary. $\alpha^j_{\rm rot}$ is the rotation angle of the jth grain with respect to the global coordinate system and $\beta^{(r)}$ is the rotation angle of the local coordinate system with respect to the same global system.

On the other hand, there is a simple phenomenological phase field approach, where the kinetic coefficient L and the gradient energy coefficient k are formulated in such a way that they reflect the anisotropy in mobility and energy of interfaces. This method has been successfully applied to describe surface energy and mobility anisotropy in modeling crystal growth.[33,39] A similar method is used in the current paper to describe grain boundary energy and mobility anisotropy. For simplicity we consider two-dimensional crystals with tilt boundaries where, excluding rigid-body translations, a grain boundary can be described by the relative orientation θ of the grains (misorientation) and the spatial orientation of the boundary ϕ with respect to a local coordinate system defined by the two contacting grains.

Using a simple dislocation model, the energy of a low angle tilt boundary ($\theta \leqslant 20^0$) between crystals with fourfold symmetry can be approximated as[40]

$$E(\theta,\phi) = E_0(|\cos(\phi)| + |\sin(\phi)|)\ \ \theta\ \ (1 - \ln(\theta/\theta_m)), \tag{3}$$

where inclination ϕ is measured from the symmetric tilt boundary (see Fig. 1), θ_m is the misorientation for which energy is maximum and E_0 is a constant. It can be shown that the gradient coefficient k and the grain boundary energy are related to each other by the simple relationship: $k \propto E^2(\theta,\phi)$.[41] On the other hand, for the Ginzburg-Landau equations (1) to be properly defined, the gradient coefficient k should be a differentiable function of inclination.[42] To satisfy this condition, in the simulations grain boundary energy can be taken in the form

$$E(\theta,\phi) = E_0(1 - \delta_E \cos(4\phi))\ \ \theta\ \ (1 - \ln(\theta/\theta_m)), \tag{4}$$

where δ_E is a phenomenological parameter controlling the degree of anisotropy. For example, by taking $\delta_E = 0.24$ one gets the same anisotropy ratio as in Eq. (4), where the anisotropy ratio r is defined as a ratio of the largest value for the grain boundary energy to the smallest one at a fixed misorientation θ_0: $r = \max[E(\theta_0,\phi)]/\min[E(\theta_0,\phi)]$. It should

be noted that the inclination dependence in Eq. (4) is similar to the one used in the phase field simulations of the solidification process.[33]

In contrast to grain boundary energy anisotropy, mobility anisotropy is more difficult to characterize. Our knowledge of mobility anisotropy is limited by the lack of experimentally available information. Qualitatively, in pure materials the higher is the defect concentration at the grain boundary the higher its energy as well as its mobility. Thus, in our simulations we assume grain boundary mobility, which is represented by the kinetic coefficient L, to have the same form as the one for grain boundary energy [see Eq. (4)]

$$L(\theta,\phi)=L_0(1-\delta_L\cos(l\phi))\quad \theta\quad (1-\ln(\theta/\theta_m)) \tag{5}$$

but with a different phenomenological parameter δ_L and a different constant L_0. Here l represents the symmetry of the grain boundary mobility with respect to inclination. By varying both δ_E and δ_L one can change the anisotropy ratios and investigate the effect of the interplay between energy anisotropy and mobility anisotropy on grain growth.

It should be noted that the exact form of the free energy density function $f_0(\eta_i)$ is not important as long as it provides the correct topology of the free energy functional, which contains a large number of energetically degenerate potential wells at the points in the η space located at $(\eta_1,\ldots,\eta_p)=(\pm 1,\ldots,0),\ \ldots,\ (0,\ldots,\pm 1)$, where it is assumed that $|\eta_i|=1$ inside the ith grain type (grain with a particular spatial orientation) and 0 otherwise. A simple function that satisfies these requirements can be written in the form

$$f=\sum_{i=1}^{p}\left[-\frac{a_1}{2}\eta_i^2+\frac{a_2}{4}\eta_i^4\right]+\frac{a_3}{2}\sum_{i=1}^{p}\sum_{j>i}\eta_i^2\eta_j^2, \tag{6}$$

where a_1, a_2, a_3 are positive constants.

In the simulations the grain boundary misorientation has been considered to be in the range $0<\theta<\Theta$, where $\Theta<\theta_m$ and θ_m is the value of the misorientation for which the energy $E(\theta)$ or the mobility $L(\theta)$ reaches its maximum, i.e., $E(\theta_m)=\max[E(\theta)]$. Misorientation θ_{ij} of the boundary between grains i and j is calculated as $\theta_{ij}=|i-j|\Theta/(p-1)$, where $i,j=0,\ldots,p-1$ and p is the total number of order parameters used in the computer simulation. The other variable that distinguishes a grain boundary is its inclination. To determine the boundary inclination we use the fact that the boundaries in the phase field approach are characterized by the gradients in the field variables. Introducing a new variable proportional to $\vec{\nabla}\eta$, which is nonzero only at grain boundaries with a direction normal to the boundary, one can describe the spatial orientation of the grain boundaries. It should be noted that the inclination defined this way is measured with respect to the reference (global) coordinate system, in contrast to Eq. (4), where the inclination ϕ is defined with respect to the symmetric tilt boundary. The orientation of the symmetric tilt boundary with respect to the global reference frame is given by $\phi_{ij}^{(0)}=(i+j)\Theta/(2(p-1))$. Then the inclination ϕ, which appears in Eq. (4) can be calculated as

$$\phi-\pi/2=\arctan\left(\frac{\nabla_y\eta}{\nabla_x\eta}\right)-\phi^{(0)}, \tag{7}$$

where the inclination ϕ is measured from a tangential to the grain boundary (Fig. 1), η could be either η_i or η_j. Here we assume that rotation of the grain boundary by 180° does not change its properties.

The following values for the phenomenological parameters in Eq. (6) have been used in our simulations: $a_1=1.0$, $a_2=1.0$, and $a_3=2.0$. In order to normalize the value of the grain boundary energy to unity, in Eq. (4) the constant E_0 has been chosen in the form $E_0=1/(1+\delta_E)$. Similarly, to normalize the grain boundary mobility function to unity, constant L_0 is taken to be $1/(1+\delta_L)$. In the simulations, Ginzburg-Landau equations (1) have been discretized on a unit square lattice with $dt=0.1$.

III. GROWTH KINETICS OF A SINGLE GRAIN

A. Single-sided island grain

We start our analysis with a brief description of the shrinkage of an island grain in an infinite matrix. Such a grain has no vertices and all possible inclinations present, i.e. $0\leqslant\phi<2\pi$. Below it will be referred to as a single-sided grain. A complete and detailed analysis can be found in our previous work.[43] Here we present only the main results. When only the grain boundary energy is anisotropic, an initially circular grain relaxes to the appropriate Wulff shape and then shrinks in a self-similar manner. In agreement with theoretical predictions of Taylor and Cahn,[44] the area of the island grain changes linearly with time. Moreover, relatively small anisotropy in the boundary energy ($r_E=1.1$) can produce strongly anisotropic grain shapes. On the other hand, if energy is isotropic but the mobility is anisotropic, it can be shown analytically that the shrinkage rate of a single sided grain is time independent (see the Appendix). However, in order to get similar anisotropy in the grain shape, a much larger anisotropy ratio in grain boundary mobility is required ($r_L\sim 10$). Based on recent computer simulations[45] as well as experimental studies,[6,46,47] mobility anisotropy can be orders of magnitude larger than the energy anisotropy. Thus, one can expect that the shapes of grains are in general determined by the interplay between the energy and mobility anisotropy of grain boundaries. In our simulations, an island grain with a quasi-eightfold shape has been observed, which would otherwise assume a fourfold shape if either energy or mobility dominates. In order to achieve a better understanding of these effects, it is important to first understand the effects of energy and mobility separately. In this paper we focus on the effect of anisotropy in grain boundary mobility. The effect of the energy anisotropy as well as their interplay will be presented elsewhere.[32]

B. Single grain with triple junctions

In this section we discuss the growth (or shrinkage) kinetics of grains with triple junctions in the presence of anisotropy in the mobility coefficient. Throughout the section the grain boundary energy is considered to be isotropic. As a

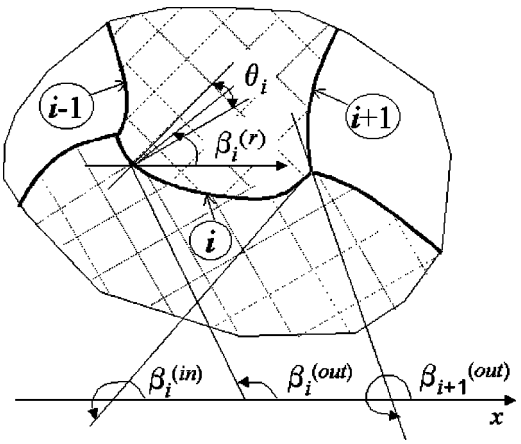

FIG. 2. Schematic drawing of an arbitrary-sided grain with triple junctions. Labels $(i-1),i,(i+1)$ denote different sides of the grain. $\beta_i^{(\mathrm{out})}$ and $\beta_i^{(\mathrm{in})}$ are the outgoing and incoming inclinations of the ith grain side at the triple junctions, which are measured in the global coordinate system.

result any multi-junction that has more than three lines meeting at the vertex will be energetically unstable and will immediately break up into several triple junctions with an angle of 120° between the incoming lines.[13]

Decades ago von Neumann[48] and later Mullins[29] showed that the growth rate of a single grain with triple junctions is time independent if both energy and mobility of the grain boundaries are isotropic, which is now referred to as the von Neumann–Mullins relationship. Moreover, they demonstrated that grains with fewer than six sides shrink and those with more than six sides grow at a constant rate that is only a function of mobility and energy coefficients. As we discussed in the previous section, mobility anisotropy for a single grain without triple junctions (single sided grain) results in the same shrinkage kinetics as in the isotropic limit, i.e., $A-A_0 \sim t$. There is, however, a major difference between a single-sided and a multiple-sided grain, i.e., the introduction of triple junctions results in a discontinuous change in grain boundary inclination at a vertex, which, as will be shown below, may dramatically change the grain growth kinetics.

Following the analysis of Mullins[29] for the isotropic case, the growth rate of an n-sided grain may be written in the following form:

$$\frac{dA_n}{dt} = -k\sum_{i=1}^{n} \int_{\beta_i^{(\mathrm{out})}}^{\beta_i^{(\mathrm{in})}} L_i(\theta_i,\beta)\,d\beta, \tag{8}$$

where $\beta_i^{(\mathrm{out})}$ and $\beta_i^{(\mathrm{in})}$ are the inclinations of the ith side of a grain with n sides outgoing from and incoming to the two triple junction at both ends of the ith side (see Fig. 2). θ_i is the grain boundary misorientation angle of the ith boundary and k is the gradient energy coefficient in the free energy functional (2). It should be noted that the grain boundary inclinations, introduced in Fig. 2, are defined with respect to a fixed global coordinate system. However, each boundary has different misorientation and its inclination should be defined in a local coordinate system which serves as a reference for the measurement of the inclination (e.g., deviation from the orientation of the symmetrical tilt boundary). Thus, the boundary mobility L_i has a subscript index i, which represents the fact that mobility of each of the boundaries is defined in its own coordinate system. We will denote $\beta_i^{(r)}$ as the angle between the local coordinate system at a particular boundary and the global (reference) system. Then, the ''true'' inclination of the boundary, ϕ, is defined as $\phi=\beta-\beta_i^{(r)}$. Introducing $\phi_i^{(out)}=\beta_i^{(out)}-\beta_i^{(r)}$ and $\phi_i^{(in)}=\beta_i^{(in)}-\beta_i^{(r)}$ the expression for the growth rate of the n-sided grain could be rewritten in the following form:

$$\frac{dA_n}{dt} = -k\sum_{i=1}^{n} \int_{\phi_i^{(\mathrm{out})}}^{\phi_i^{(\mathrm{in})}} L(\theta_i,\phi)\,d\phi, \tag{9}$$

where L is the mobility of the boundary as a function of its misorientation and local inclination.

Generally speaking there is an infinite number of ways for choosing the local coordinate system and the particular choice could vary from system to system depending on the underlying crystallography of the material as well as on the details of the mobility function. For example, in the case of crystals of cubic lattice, the most convenient choice for the local system is the one that coincides with the symmetric tilt boundary (see Fig. 1). As we will show later, this definition of the local system provides the simplest form for the mobility L as a function of local inclination.

Using Eq. (9) we deduce that there are two ways a single n-sided grain may have a constant growth rate. The first occurs if the grain grows (or shrinks) in a self-similar manner, i.e., maintains shape while the area changes. Then both $\phi_i^{(\mathrm{out})}$ and $\phi_i^{(\mathrm{in})}$ are independent of time for all i. However, this is a very rare case for an arbitrary n-sided grain in a polycrystalline aggregate. Another possibility for dA_n/dt to be constant occurs if the overall sum in Eq. (9) is time independent, although the limits of the integration might change with time. It can be easily shown that this condition is always satisfied in the isotropic case, i.e., when the grain boundary mobility $L=\mathrm{const}$.[29] However, if the mobility is anisotropic such a condition is rarely met, thus, generally speaking, the growth rate of a single grain with triple junctions is time dependent.

To validate these predictions we perform a computer simulation using the phase-field approach described in Sec. II. For a simple and vivid demonstration of the fact that growth of a single grain with triple junctions and anisotropic boundary mobility is nonlinear in time, in the simulation we have considered a system consisting of two contacting grains embedded in an infinite matrix. Even though each of the grains has only two sides, the general conclusion should be equally applicable to any n-sided grain.

In the simulation, the grain boundary mobility has been assumed to have a twofold symmetry with respect to inclination, i.e., Eq. (5) with $l=2$, where the inclination ϕ is measured from the symmetric tilt boundary and the local coordinate system coincides with the symmetric tilt boundary (see Fig. 1). The following values of the input parameters have been used in the simulations: $\theta_m=10°$, $\Theta=5°$ and the

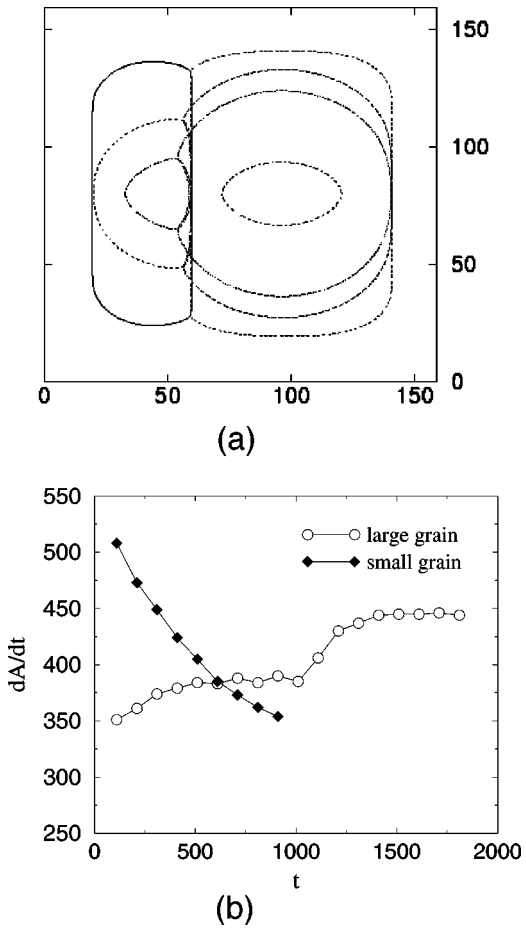

FIG. 3. (a) Microstructural evolution and (b) shrinkage rate in a system of two grains in an infinite matrix with anisotropic grain boundary mobility with twofold symmetry.

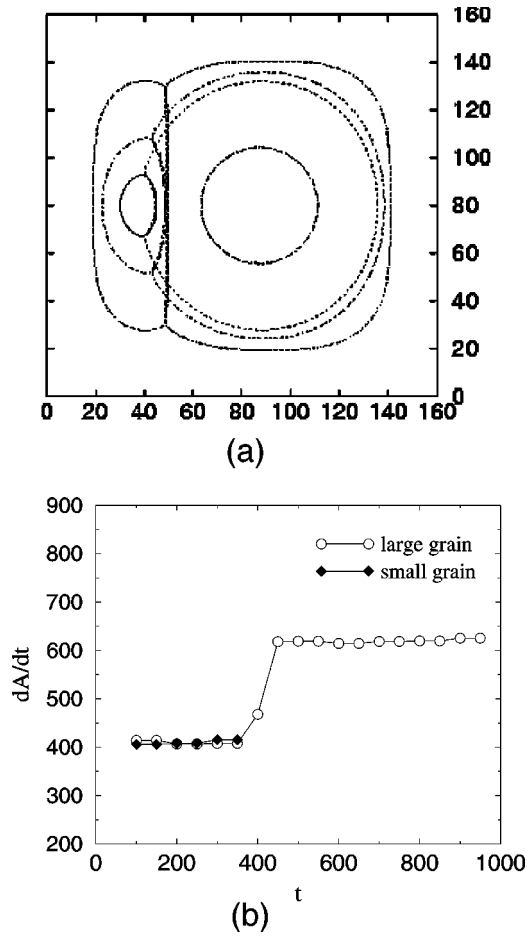

FIG. 4. (a) Microstructural evolution and (b) shrinkage rate in a system of two grains in an infinite matrix with isotropic boundary properties.

anisotropy factor $\delta_L = 0.9$, which gives an anisotropy ratio of $r_L = 19$. $\Theta = 5°$ implies that the maximum deviation of the local coordinate systems orientation from each other is 5°, e.g., as in a textured grain structure.

Results of the simulations are presented in Fig. 3. The simulation was started from two rectangular grains of different sizes in contact. Since $\phi = \pi/2 + \pi n$ is the fastest growth direction the shapes of both grains become more and more elongated along this direction. Accompanying the shape change, the vertices at the triple junctions rotate [Fig. 3(a)]. It can be seen from Fig. 3(b) that when both grains are present, each of them shrinks nonlinearly. However, as soon as the smaller one disappears ($t \approx 1200$), the triple junctions disappear as well and the remaining grain shrinks at a constant rate, in agreement with the results presented in Sec. III A.

These results demonstrate that in contrast to the isotropic case[29] or the case of a single-sided grain with mobility anisotropy, the introduction of vertices in systems with anisotropic boundary mobility results in completely different grain growth kinetics, i.e., the growth rate of individual grains is no longer time independent. For comparison, results obtained from the same initial microstructure but with isotropic boundary properties are shown in Fig. 4.

IV. POLYCRYSTALLINE AGGREGATE

Results from the previous section suggest that introduction of mobility anisotropy may change the growth kinetics of a single grain in a polycrystalline aggregate, although the quantity usually calculated in a polycrystalline aggregate is the growth rate of the average grain area, rather than the growth rate of a single grain. In this section we evaluate the effect of grain boundary mobility anisotropy on both the average growth rate of grains in a given ''topological class'' as well as the growth rate of the averaged grain area. Here, by ''topological class p'' we mean class of grains with p sides. In addition we will compute a number of distribution functions, such as size and edge distributions, which are usually calculated in grain growth analysis and compare them to the results obtained in the isotropic limit.

A. Small misorientation limit

Computer simulations were performed on a 512×512 square lattice with 36 order parameters, which describe 36 possible grain orientations. The simulations were started from the isotropic polycrystalline microstructure containing ~ 1000 grains, which were obtained from nucleation and growth of crystals from the liquid phase in an isotropic sys-

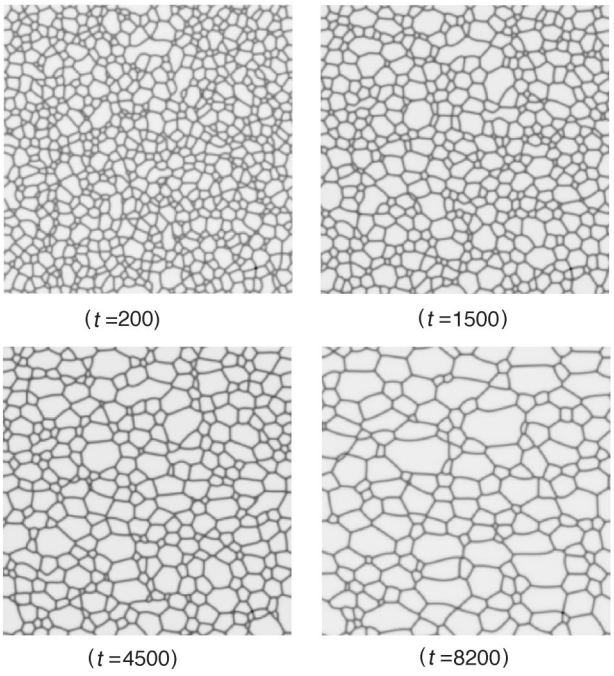

FIG. 5. Typical microstructural evolution obtained from computer simulation of grain growth in a system with isotropic grain boundary energy and anisotropic boundary mobility with twofold symmetry with respect to inclination ϕ. The system is considered to be textured, i.e., the range of misorientations involved in the simulation is $0<\theta<5°$.

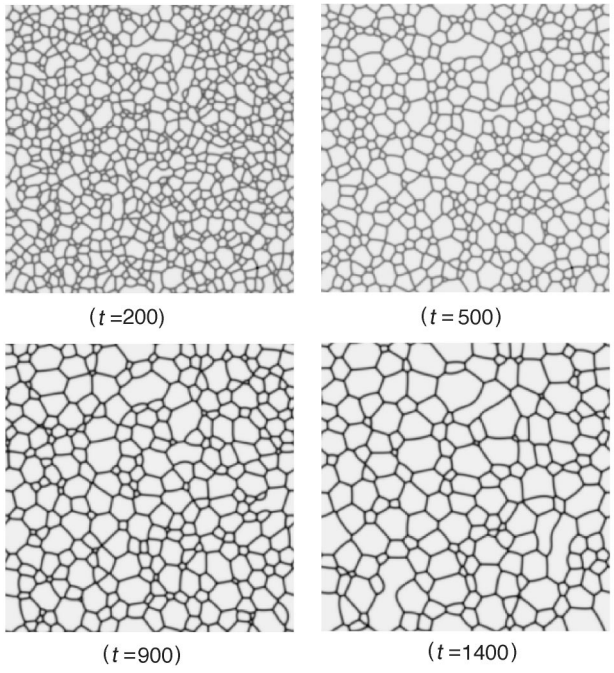

FIG. 6. Typical microstructural evolution obtained from computer simulation of grain growth in an isotropic system.

tem. The grain boundary mobility function has been assumed to have a twofold symmetry with respect to inclination, i.e., using Eq. (5) with $l=2$, where the normalization factor L_0 is chosen so that $\max[L(\theta,\phi)]=1/L_0$. To satisfy the condition of small misorientation, the following values of the parameters have been used in the simulations: $\theta_m=10°$, $\Theta=5°$ and the anisotropy factor $\delta_L=0.9$. In the simulations the grain boundary misorientation is considered to be in the range $0<\theta<\Theta$. Such a choice of the mobility function results in grain boundaries with their normal parallel to $\phi=\pi/2$ direction having the fastest mobility. Since the local and global coordinate systems almost coincide with each other, one can assume that the direction $\pi/2$ is with respect to the global system and the expected microstructure should then consist of horizontally elongated grains. Results of our simulations are presented in Fig. 5. For comparison, the results obtained from the same initial microstructure but with isotropic boundary properties are shown in Fig. 6.

Grain shape anisotropy. Comparing these two series of results, it is clear that in the anisotropic case grain shape anisotropy develops. To measure this effect quantitatively, we calculate the inclination distribution function, which represents the fraction of the grain boundary length with a particular inclination (see Fig. 7). Due to the twofold symmetry and inversion symmetry of the mobility function with respect to inclination, here we plot only the data from the first quadrant ($0<\phi<90°$). At the beginning the distribution is uniform, i.e., there is no preferred orientation in the system. As the simulation proceeds the fraction of the boundary length with inclinations $\phi<10°$ starts to grow at the expense of the boundaries with inclinations $\phi\sim 90°$, indicating the development of grain shape anisotropy.

A similar conclusion can be reached by analyzing the ratio of the average cord lengths in the horizontal and vertical directions, $\bar{d}_x/\bar{d}_y$, as a function of time. Initially, the microstructure is isotropic and the ratio is equal to unity. As the system evolves the shape of the grains starts to change and the ratio $\bar{d}_x/\bar{d}_y$ becomes time dependent (see Fig. 8). More importantly, this demonstrates the fact that the microstructure is not evolving in a statistically ''self-similar'' (scaling) manner. By statistical ''self-similarity'' we mean that all configurations have identical statistics when transformed to the same linear scale by uniform magnification.[10] This is in agreement with the earlier predictions of Mullins that self-similarity may not hold when the boundary properties (such

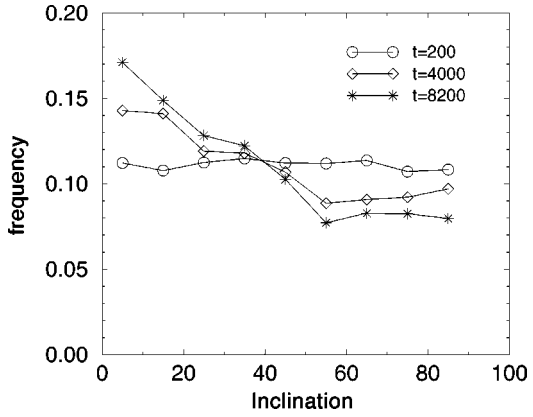

FIG. 7. Inclination distribution obtained from computer simulation of the microstructural evolution in the textured system with anisotropic grain boundary mobility, shown in Fig. 5.

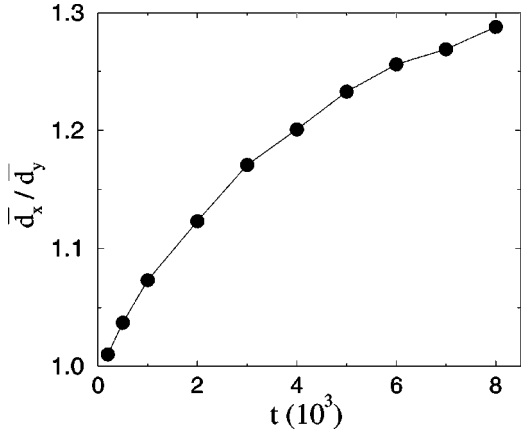

FIG. 8. Time evolution of the mean grain intercepts ratio $(\overline{d_x}/\overline{d_y})$ in a textured polycrystalline system with grain boundary mobility anisotropy, shown in Fig. 5.

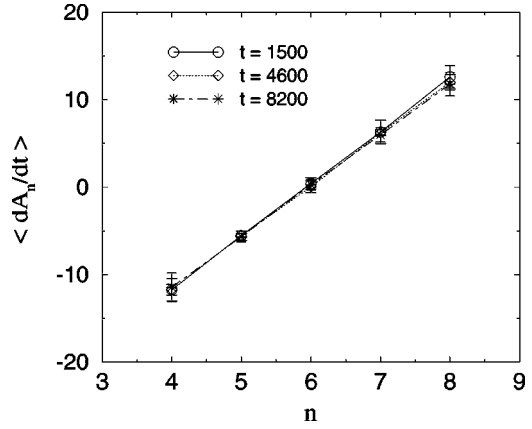

FIG. 9. Average growth rate of the grains in different topological classes as a function of the topological class. The data is averaged over three simulations.

as energy and/or mobility) are anisotropic.[10] However, as argued below, in the case of grain growth in textured materials with mobility anisotropy, even though self-similarity is no longer satisfied, the average area still grows linearly with time.

In addition we have looked at both $\overline{d_x}$ and $\overline{d_y}$ distributions, where each distribution is normalized by its own average value. It has been found that both distributions are almost time independent, suggesting that the breaking of self-similarity takes place in the simplest possible way, i.e., only through change in the grain shape anisotropy, as shown below by the difference in the growth exponents for $\overline{d_x}$ and $\overline{d_y}$. It should be noted that absence of self-similarity is not a consequence of the initial isotropic microstructure. We performed a number of simulations where the microstructure has been grown anisotropically from liquid phase with anisotropic boundary mobility. It has been observed that after the full crystallization of the system, self-similarity has not been achieved even after tenfold increase in the average grain area.

Average growth rate of n-sided grains. We start with the calculation of the average growth rate of grains in a given topological class. Averaging Eq. (9) over the topological class, the growth rate of *n*-sided grains can be written as

$$\left\langle \frac{dA_n}{dt} \right\rangle = \left\langle \frac{dA_n}{dt} \right\rangle_0 + \delta \left\langle \frac{dA_n}{dt} \right\rangle, \tag{10}$$

where the first term is the analog of von Neumann-Mullins relationship and is time independent. The second term is in general time dependent and distinguishes the behavior of the system with anisotropic boundary mobility from that of an isotropic system. Using symmetry arguments it can be shown that the second term on the right side is insignificant in the limiting cases of either textured or fully random polycrystalline systems, implying the von Neumann-Mullins relationship in those limits. Details of the derivation will be presented elsewhere.[49]

Results of the simulations are presented in Fig. 9. The calculation has been performed at three different time moments by monitoring the area change of the grains in the same topological class over a short time interval Δt. The results presented here and below are averaged over at least three simulations. First of all it can be seen that within the statistical error of the simulations all three lines coincide with each other. This indicates that the average growth rate of the grains with *n* sides is indeed time independent, which is in contrast to the time-dependent growth rate of a single grain with anisotropic boundary mobility (see Sec. III B). On the other hand, Fig. 9 shows that the relationship between the average growth rate $\langle dA_n/dt \rangle$ and the topological class *n* is linear, in agreement with our theoretical predictions. Similarly to the isotropic case, grains with $n>6$ tend to grow and with $n<6$ tend to shrink, while on average $n=6$ grains have a zero growth rate.

Size and edge distributions. Size and edge distribution are usually analyzed in the study of grain growth in addition to the average grain growth kinetics. In this study, the grain size distribution is obtained by examining the frequency of occurrence of grains with an area *A* normalized by the average grain area $\langle A \rangle$. Simulation results, corresponding to the beginning, intermediate and end of the simulations are shown in Fig. 10. It is observed that, as in the well-studied isotropic case, the normalized size distribution function has a bell-type shape and is virtually time independent. To make sure that the results are not affected by the size of the computational cell, we have repeated the simulations in a 1024 $\times$1024 system and observed the same characteristics for the size distribution function.

The edge distribution function describes the relationship between the frequency of occurrence of grains with certain number of sides f_n and the ''topological class'' *n*. The results of the simulation at several selected time moments are plotted in Fig. 11. These time moments correspond to the beginning, intermediate, and final stages of the simulations. It is observed that even though grain shape anisotropy develops, the edge distribution is almost time independent. It is also observed that as in the isotropic case, five-sided grains have higher probability of occurrence than six-sided grains. However, the average number of edges of the grains is time

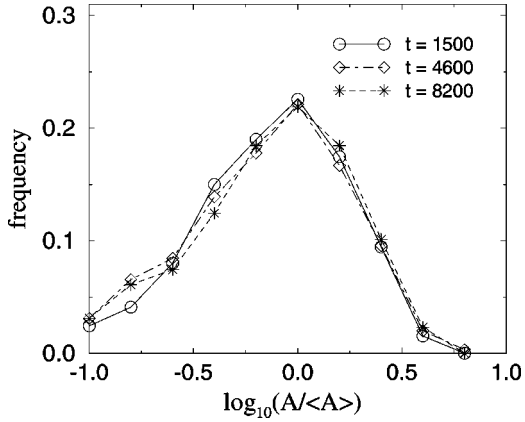

FIG. 10. Grain size distribution function at different stages of evolution in the textured polycrystalline system with anisotropic boundary mobility, shown in Fig. 5.

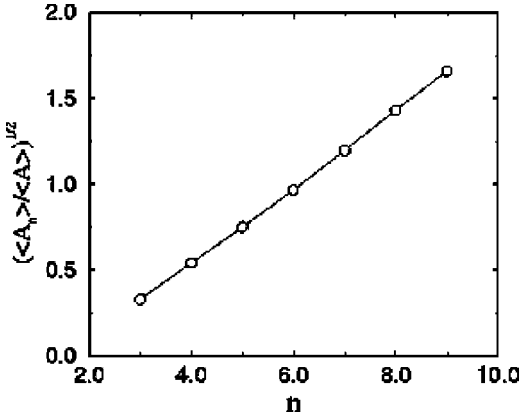

FIG. 12. Dependence of the average area of the *n*-sided grains on the ''topological class'' *n*.

invariant and equal to six, which is a direct consequence of the isotropic boundary energy (see, e.g., Ref. 50).

In addition, to compare statistical properties of the isotropic systems with the systems with anisotropic boundary mobility we compare their size and edge distributions. It is observed that in both isotropic and anisotropic cases the distributions are very similar and are independent of the particular form of the mobility function.

Lewis' law. Another topological property of interest is the relationship between the average area of the *n*-sided grains $\langle A_n \rangle$ and the ''topological class'' *n*. Results of our computer simulation are presented in Fig. 12. These results suggest that $\sqrt{\langle A_n \rangle} \sim n$, as found in previous computer simulations[11,15] as well as theoretical analysis[51,52] of grain growth in isotropic systems. On the other hand, this is in disagreement with the results obtained for the evolution of a two-dimensional cellular mosaics, which have been used for the analysis of grain growth behavior. Lewis first observed in the case of the cellular mosaics the proportionality (Lewis' law) $\langle A_n \rangle \sim (n-2)$ for the average area of *n*-sided grains.[53] Later analytical arguments for this were given by Rivier and Lissovski.[54] However, as pointed out by Weaire and Rivier,[50] on closer inspection, these problems may have dissimilarities as well, since in the analysis of Ref. 54 the edge distribution is assumed to be an arbitrary function of *n*, which satisfies certain topological constraints. On the other hand, during grain growth, the edge distribution as we have seen is unique and does not depend on the initial condition, which results in a different dependence of $\langle A_n \rangle$ on topological class number *n*. Thus, in systems with unique edge distribution functions, it may be unlikely that Lewis' law is satisfied.

Average grain area. Conventionally, to describe the overall kinetics of a coarsening process, the value of the average size(area) of domains is analyzed as a function of time. It is generally assumed that the evolution of the average grain area obeys the power law growth $\langle A \rangle \sim t^k$ and the value of *k* is usually referred to as the growth exponent. For grain growth in pure materials with both isotropic energy and mobility of grain boundaries, $k=1$. Below we analyze the implication of mobility anisotropy on the growth exponent. Results of the simulations are presented in Fig. 13. In accordance with our theoretical predictions,[49] in the extreme case of highly textured polycrystalline aggregate, average area of the grains is indeed growing linearly with time. The extracted value of the growth exponent is $k=1.00\pm0.02$.

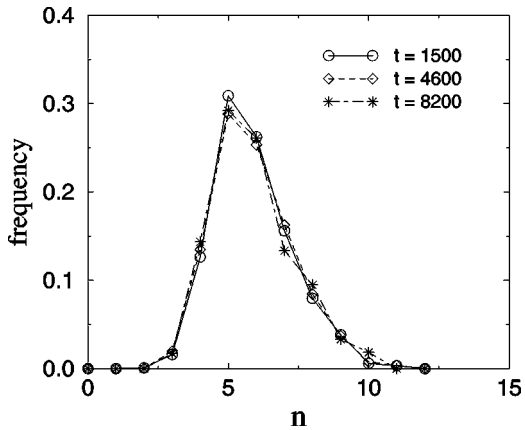

FIG. 11. Grain edge distribution function at different stages of evolution in the textured polycrystalline system with anisotropic boundary mobility, shown in Fig. 5.

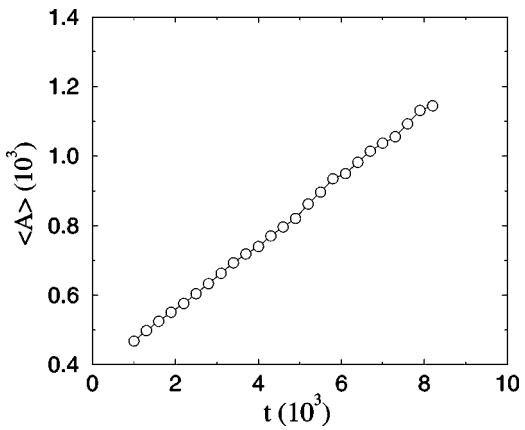

FIG. 13. Time dependence of the average grain area in the textured polycrystalline system with anisotropic boundary mobility (see Fig. 5).

In the isotropic case, due to the equiaxed shape of the grains, length scale is usually characterized by the average grain radius $\langle R\rangle \propto \langle A\rangle^{1/2}$ and grain growth kinetics is described by the growth exponent $n=k/2$. However, in the anisotropic case such a measure for the length scale is no longer applicable, because the grains are no longer equiaxed. In the small misorientation limit with twofold boundary mobility function we have shown that grains become elongated and the proper length scale in the problem is characterized by the average grain sizes in the horizontal $\overline{d_x}$ and vertical $\overline{d_y}$ directions. Similarly to $\langle R\rangle$, time evolution of each of them can be approximated as a power law, e.g., $\overline{d_x} \propto t^{n_1}$ and $\overline{d_y} \propto t^{n_2}$. Then, in the first approximation the average grain area is described as $\overline{d_x} \times \overline{d_y}$ and $n_1+n_2=1$. However, the major difference from the isotropic case is that $n_1 \neq n_2 \neq 1/2$. Indeed, from the computer simulations we obtain $n_1=0.61 \pm 0.02$ and $n_2=0.39 \pm 0.02$, which again demonstrates that in contrast to the isotropic limit microstructural evolution is no longer ''self-similar.''

Misorientation and orientation distributions. The last two quantities that we would like to discuss are the misorientation distribution, which is the fraction of grain boundaries with different misorientations and the grain orientation distribution, which is the fraction of grains with different orientations with respect to the global system. These features are widely analyzed in the studies of texturing in polycrystalline systems. The simulation is started with a textured polycrystalline aggregate where the grains with different orientations are randomly distributed throughout the system and the largest misorientation of the grain boundary is 5°. One might expect that the grain boundaries with larger misorientations are disappearing faster due to their higher mobilities, thus forming a more textured material. However, both distributions do not change with time and no further texturing in the system is observed, which is the result of constraints imposed on grain boundaries at triple junctions.

B. Fully random and intermediate cases

Fully random limit is characterized by random distribution of grains over the entire range of grain rotation angles α_{rot}. For example, for the grains with twofold symmetry, α_{rot} should be randomly distributed over the range $[0,\pi)$. If this randomness is preserved during the evolution of the polycrystalline system, the time dependent corrections to the average growth rate vanishes and the evolution of the system is isotropiclike.[49] To validate this prediction we performed computer simulations using the same set of parameters as in the small misorientation case. To satisfy the periodicity of the grain boundary mobility function over misorientation, mobility has been formulated as $L(\theta,\phi)=L_0 \sin(2\theta)[1-\delta_L \cos(2\phi)]$. To examine whether the randomness is preserved during the evolution of the system, we monitored the changes in the ''inclination distribution'' and ''misorientation distribution'' functions. Results of the simulation show that both distribution functions are indeed time independent, suggesting that randomness is preserved. In addition, no texturing has been observed in the system. As a result, average area of the grains grows linearly with time ($k=1\pm0.02$), which is in agreement with analytical predictions.

The analysis appears to be more complicated in the intermediate case. For the twofold symmetric mobility function this is the range where $0<(\alpha_{\mathrm{rot}})_{\max}<\pi$. Simulations were performed using the same grain boundary mobility function and the same parameters as used in the fully random case. A number of simulations have been carried out with the maximum grain rotation angle $(\alpha_{\mathrm{rot}})_{\max}$ equal to 11°,22°,45°, and 90°. As in the textured case, the growth rate of the average grain area has been fitted to the simple power law of the form $\langle A\rangle \propto t^k$. Simulation results suggest that deviations in the growth exponent from unity are quite small [maximum of 10% at $(\alpha_{\mathrm{rot}})_{max}=45°$] and time dependence of the average grain area is almost linear.

In addition to grain growth kinetics, size and edge distributions which characterize topological and morphological changes in a polycrystalline aggregate are also investigated. Simulation results show that, as in the small misorientation case, both distribution functions are almost time independent for all rotation angles and are very similar to the isotropic one, suggesting that anisotropy in the grain boundary mobility has a small effect on a number of statistical properties of the system during the grain growth, including size and edge distribution functions.

It should be noted that although there might be an additional influence of the initial conditions as well as of the particular form of the mobility function, as long as mobility is a smooth function of inclination, both kinetics and statistics of the system in the intermediate range are unlikely to change drastically compared to the present simulation.

V. CONCLUSIONS

We have studied dynamics, morphology and topology of grain growth with grain boundary mobility anisotropy both analytically following the analysis of Mullins for the isotropic case and numerically using a generalized phase field model that incorporates both inclination and misorientation dependence of the grain boundary mobility. It is found that the area of a single-sided island grain changes linearly with time while an arbitrary *n*-sided grain grows nonlinearly. The latter is in contrast to the isotropic case where an *n*-sided grain grows linearly with time. For a polycrystalline aggregate the average growth rate of the grains in a given topological class can be written as a sum of two terms with the first term being time independent and identical to that given by the von Neumann–Mullins result and the second time-dependent term describing the difference in grain growth kinetics between an isotropic and anisotropic system. Both theoretical analysis and computer simulations indicate that in the two extreme cases of textured and randomly oriented grain structures the nonlinear corrections are negligible and the average area of grains in a polycrystalline aggregate grows linearly with time. For cases in between the two extreme cases, the computer simulation study has shown that the average grain area indeed grows nonlinearly with time. However the corrections to the growth exponent *k* are rather small (e.g., no more than 10%). In addition it has been

shown that independently of the cases considered, both edge and size distributions are time independent and similar to the ones obtained in the isotropic limit. It has also been argued that since the edge distribution is a unique function and does not depend on the initial configuration, as in the isotropic case, Lewis' law may not be satisfied. Based on the above results it may be concluded that even though anisotropy in grain boundary mobility changes kinetics of a single grain in a polycrystalline aggregate, the average grain growth kinetics as well as size and edge distributions are very similar to the results observed in the isotropic systems.

Even though the average grain area grows linearly with time and grain size and edge distributions are time-independent and similar to the ones observed in the isotropic system, strong grain shape anisotropy develops in the textured polycrystalline system with mobility anisotropy. Both mean grain shape aspect ratio and grain boundary inclination distribution functions are found to be strongly time-dependent, which obviously violates the self-similarity criterion. Therefore, one may conclude that even though there are many characteristics associated with self-similarity such as linear growth kinetics and time-independent size and edge distributions, just by examining one or several of these characteristics obtained either from experimental or simulation data one may not be able to predict whether the grains grow in a self-similar mode or not. On the other hand, statistical self-similarity may not be necessary to lead to linear growth kinetics in certain kinds of systems.

ACKNOWLEDGMENTS

We gratefully acknowledge the financial support of NSF under Grant No. DMR-9703044 (A.K. and Y.W.) and NSF Center for Industrial Sensors and Measurements under Grant No. EEC-9523358 (A.K. and B.R.P.).

APPENDIX

In this appendix we show that the shrinkage rate of an island grain in an infinite matrix with anisotropic grain boundary mobility is time independent, as observed in the isotropic case. In the isotropic case, when both gradient energy coefficient k and kinetic coefficient L in the Ginzburg-Landau equations (1) are constant, Allen and Cahn[55] have shown that, similarly to the sharp-interface approach, the velocity of the boundary can be written as

$$v = -\kappa k L, \tag{A1}$$

where κ is the mean local curvature. Here, boundary velocity is defined as the velocity of an iso-η surface in the direction normal to itself, i.e., in the direction parallel to $\nabla\eta$. However, it should be noted that this expression for v is valid when the principal radii of curvature are large compared to the thickness of the boundary.

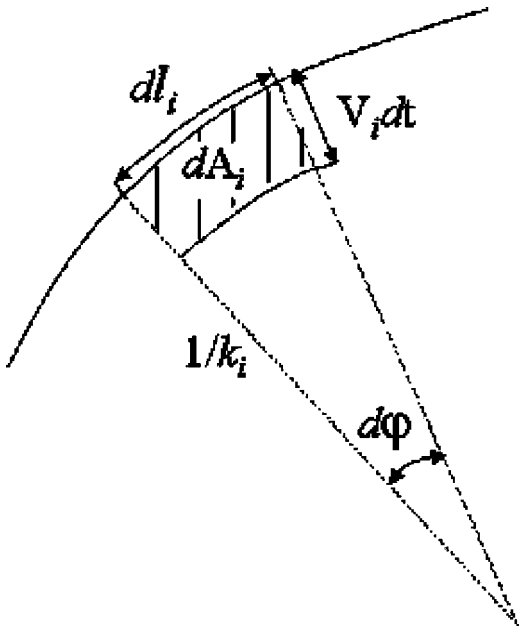

FIG. 14. Schematic drawing of the grain boundary segment dl_i, moving with velocity v_i in the direction normal to the boundary and changing the grain area by dA_i during the time interval dt. κ_i is the local curvature of the segment dl_i.

Following the exact mathematical procedure formulated in Refs. 55 and 56 it can be shown that if kinetic coefficient L is not a constant but a function of misorientation and inclination, Eq. (A1) still holds, e.g., $v = -\kappa k L(\theta,\phi)$. This means that anisotropy in the mobility coefficient does not change the local grain boundary kinetics. It should be noted that if grain boundary coefficient k is anisotropic, $k = k(\theta,\phi)$, Eq. (A1) is no longer valid.

To calculate the shrinkage rate of the island grain we divide the the entire grain boundary into small segments dl_i, each having local velocity v_i and local curvature κ_i (Fig. 14). Then, the overall shrinkage rate is calculated as a sum of the contributions from each of the segments dl_i. Assuming that the segments are infinitesimally small

$$\frac{dA}{dt} = -\oint \kappa k L(\theta,\phi)\ dl, \tag{A2}$$

where the integration is performed over the entire grain boundary, and using the relationship $\kappa\ dl = d\phi$, it can be deduced that

$$\frac{dA}{dt} = -2\pi k \langle L(\theta,\phi)\rangle_\phi, \tag{A3}$$

where $\langle \ldots \rangle_\phi$ denotes averaging over the grain boundary inclinations. Equation (A3) demonstrates that the shrinkage rate of the island grain with boundary mobility anisotropy is indeed time invariant as observed in the isotropic case.

[1] D. Weaire and S. McMurry, Solid State Phys. **50**, 1 (1997).
[2] H.J. Frost and C.V. Thompson, Curr. Opin. Solid State Mater. Sci. **1**, 361 (1996).
[3] V.E. Fradkov and D. Udler, Adv. Phys. **43**, 739 (1994).
[4] J. Stavans, Rep. Prog. Phys. **56**, 733 (1993).
[5] J.D. Powers and A.M. Glaeser, Interface Sci. **6**, 23 (1998).
[6] *Grain-Boundary Structure and Kinetics*, Proceedings of the ASM Materials Science Seminar, Milwaukee, Wisconsin (American Society of Metals, Metals Park, OH, 1980).
[7] G. Gottstein and L.S. Shvindkerman, *Grain Boundary Migration in Metals. Thermodynamics, Kinetics, Applications* (CRC Press, Boca Raton, FL, 1999).
[8] S.J. Bennison and M.P. Harmer, J. Am. Ceram. Soc. **66**, C-90 (1983).
[9] W.A. Kaysser, M. Sprissler, C.A. Handwerker, and J.E. Blendell, J. Am. Ceram. Soc. **70**, 339 (1987).
[10] W.W. Mullins, Acta Metall. Mater. **46**, 6219 (1998).
[11] P.S. Sahni, G.S. Grest, M.P. Anderson, and D.J. Srolovitz, Phys. Rev. B **28**, 2705 (1983); Acta Metall. **32**, 783 (1984); **32**, 793 (1984).
[12] A.C.F. Cocks and S.P.A. Gill, Acta Metall. Mater. **44**, 4765 (1996).
[13] H.V. Atkinson, Acta Metall. **36**, 469 (1988).
[14] L.-Q. Chen and W. Yang, Phys. Rev. B **50**, 15 752 (1994).
[15] D. Fan and L.-Q. Chen, Acta Metall. Mater. **45**, 611 (1997); **45**, 1115 (1997).
[16] G. Frantziskonis and P.A. Deymier, Modell. Simul. Mater. Sci. Eng. **8**, 649 (2000).
[17] V.Yu. Novikov, Acta Metall. Mater. **47**, 1935 (1999).
[18] G. Abbruzzese and K. Lücke, Acta Metall. **34**, 905 (1986).
[19] H. Eichelkraaut, G. Abbruzzese, and K. Lücke, Acta Metall. **36**, 55 (1988).
[20] F.J. Humphreys, Acta Metall. Mater. **45**, 4321 (1997).
[21] K. Mehnert and P. Klimanek, Scr. Mater. **35**, 699 (1996).
[22] G.S. Grest, D.J. Srolovitz, and M.P. Andreson, Acta Metall. **33**, 509 (1985).
[23] N. Ono, K. Kimura, and T. Watanabe, Acta Metall. Mater. **47**, 1007 (1999).
[24] W. Yang, L.-Q. Chen, and G. Messing, Mater. Sci. Eng., A **195**, 179 (1995).
[25] Z.-X. Cai and D.O. Welch, Philos. Mag. B **70**, 141 (1994).
[26] W.W. Mullins and J. Vinals, Acta Metall. Mater. **41**, 1359 (1993).
[27] W.T. Read, Jr., *Dislocations in Crystals* (McGraw-Hill, New York, 1953), p. 173.
[28] E.A. Holm, A.D. Rollet, and D.J. Srolovitz, in *Computer Simulation in Materials Science. Nano/Meso/Macroscopic Space and Time Scales*, Vol. 308 of *NATO Advanced Study Institute, Series E: Applied Sciences*, edited by H.O.Kirchner, L.P. Kubin, and V. Pontikis (Kluwer Academic, Boston, 1996), p. 373.
[29] W.W. Mullins, J. Appl. Phys. **27**, 900 (1956).
[30] W.W. Mullins, J. Appl. Phys. **59**, 1341 (1986).
[31] W.W. Mullins, Scr. Metall. **22**, 1441 (1988).
[32] A. Kazaryan, Y. Wang, and B.R. Patton (unpublished).
[33] For a recent review, see A. Karma and W.-J. Rappel, Phys. Rev. E **57**, 4323 (1998).
[34] For a recent review, see Y. Wang and L.-Q. Chen, *Methods in Materials Research* (Wiley, New York, 2000); JOM **48**, 13 (1996).
[35] A.G. Khachaturyan, Philos. Mag. A **74**, 3 (1996).
[36] R.J. Braun, J.W. Cahn, G.B. McFadden, and A.A. Wheeler, Philos. Trans. R. Soc. London, Ser. A **355**, 1787 (1997); Acta Metall. Mater. **46**, 1 (1998).
[37] R. Kobayashi, J.A. Warren, and W.C. Carter, J. Cryst. Growth **211**, 18 (2000); Physica D **140**, 141 (2000).
[38] M.T. Lusk, Proc. R. Soc. London, Ser. A **455**, 677 (1999).
[39] J.A. Warren and W.J. Boettinger, Acta Metall. Mater. **43**, 689 (1995).
[40] W.T. Read and W. Shockley, Phys. Rev. **78**, 275 (1950).
[41] J.W. Cahn and J.E. Hilliard, J. Chem. Phys. **28**, 258 (1958).
[42] G.B. McFadden, A.A. Wheeler, R.J. Braun, and S.R. Coriell, Phys. Rev. E **48**, 2016 (1993).
[43] A. Kazaryan, Y. Wang, S.A. Dregia, and B.R. Patton, Phys. Rev. B **61**, 14 275 (2000).
[44] J.E. Taylor and J.W. Cahn, Physica D **112**, 381 (1998).
[45] M. Upmanyu, D.J. Srolovitz, L.S. Shvindlerman, and G. Gottstein, Acta Metall. Mater. **47**, 3901 (1999).
[46] Y. Huang and F.J. Humphreys, Acta Metall. Mater. **48**, 2017 (2000).
[47] V.Yu. Novikov, *Grain Growth and Control of Microstructure and Texture in Polycrystalline Materials* (CRC Press, Boca Raton, FL, 1998).
[48] J. von Neumann, *Metal Interfaces* (American Society of Metals, Cleveland, OH, 1952), p. 108.
[49] A. Kazaryan, Y. Wang, and B.R. Patton (unpublished).
[50] D. Weaire and N. Rivier, Contemp. Phys. **25**, 59 (1984).
[51] G. Abbruzzese, I. Heckelmann, and K. Lücke, Acta Metall. Mater. **40**, 519 (1992).
[52] K. Lücke, I. Heckelmann, and G. Abbruzzese, Acta Metall. Mater. **40**, 533 (1992).
[53] F.T. Lewis, Anat. Rec. **38**, 341 (1928).
[54] N. Rivier and A. Lissovski, J. Phys. A **15**, L143 (1982).
[55] S.M. Allen and J.W. Cahn, Acta Metall. **27**, 1085 (1979).
[56] D. Fan and L.-Q. Chen, Philos. Mag. Lett. **75**, 187 (1997).